Special Issue on Chemistry

Green Synthesis of Zirconium Oxide Nanoparticles using *Aloe vera* Extract and their Photocatalytic Application

R. Gowthami and T. Ezhilarasu

Issue Editor
Dr. A. Manikandan

Research Journal of Agricultural Sciences
An International Journal

P- ISSN: 0976-1675
E- ISSN: 2249-4538

Volume: 13
Issue: Special

Res. Jr. of Agril. Sci. (2022) 13(S): 059–063

CARAS

Res. Jr. of Agril. Sci. (2022)
13(Special): 059–063

ISSN: 0976-1675 (P)
ISSN: 2249-4538 (E)

www.rjas.org

Full Length Research Article

Green Synthesis of Zirconium Oxide Nanoparticles using *Aloe vera* Extract and their Photocatalytic Application

R. Gowthami*[1] and T. Ezhilarasu[2]

Received: 04 Dec 2021 | Revised accepted: 10 Feb 2022 | Published online: 25 Feb 2022

A B S T R A C T

Plant extract was used to make ZrO_2 nanoparticles in a green method. ZrO_2 nanoparticles were made using zirconium, Aloe vera plant extract, and DI water. Separate amounts of *Aloe vera* plant extract and zirconium oxynitrate were dissolved in distilled water and stirred for 30 minutes. The *Aloe vera* plant extract is applied and agitated in the zirconium oxynitrate solution, then kept in a microwave oven to promote powder formation. FTIR spectroscopy, SEM, TEM, and photocatalytic experiments have all been used to characterize the materials. The XRD measurements revealed that the crystallite size of ZrO_2 nanoparticles is 15 nm. Optical studies revealed the when exposed to visible light, the nanoparticles successfully destroy the methyl orange (MO) dye. The photocatalytic experiments revealed an 88 percent degradation efficiency after 120 minutes of irradiation.

***Key words*:** Plant extract, *Aloe vera*, ZrO_2 nanoparticles, FTIR spectroscopy, SEM, TEM

Nanotechnology is a rapidly increasing area of importance and interest that encompasses a wide range of scientific topics. It is concerned with nanometer-scale materials or structures, which typically range from sub-nanometers to several hundred nanometers in size. One nanometer is 10-3 micrometres (10-9 metres). It is concerned with single nano-objects, their derived materials and devices, as well as processes occurring in the nanometer range. Nanomaterials are materials whose main physical features are dictated by the nanoobjects they contain [1-7]. Their optical and electrical properties are investigated in transparent devices, fuel cells and photocatalysts [8-10]. Nanostructured materials meet all of the requirements. Nanomaterials must be crystalline for efficient photocatalytic action, which means they must be grown at high temperatures or at extremely low rates [11-13]. When ZrO_2 is synthesized, it usually results in amorphous forms.

ZrO_2, which is also a common pottery element, is commonly utilised as a catalyst [14], a sorbent, an oxygen sensor, and a solid oxide fuel cell [15-20]. Their catalytic processes, composition, grid defaults, and shape are all affected by ZrO_2. Due to a huge energy gap and high negative values of the conductivity belt potential, it can be employed as a photocatalyst for creating hydrogen by decomposing water [21-25]. In illuminated with 365 nm wavelength light, photocatalytic activity on methyl orange (MO) dye was also observed. They discovered that when the ZrO_2 nanostructure was added, MO was easily reduced at higher pH values. The rate of breakdown is faster for ZrO_2 nanotubes with a larger diameter [26]. Because of the presence of the impurity band at around 320 nm in ZrO_2, photocatalytic activities were reported [27-32].

ZrO_2 nanostructures have been employed as a photocatalyst for the degradation of numerous dyes, but a systemic examination of ZrO_2 nanostructures photocatalytic on MO dye of varied sizes and crystalline phases may yet to be addressed [33-35]. Monoclinical (below 1170 degrees Celsius), tetragonal (between 1170 and 2370 degrees Celsius), and cubic (beyond 2370 degrees Celsius) are the three crystalline structures of ZrO_2. In addition, cubic (480 cm-1) and monoclinic (270 cm-1) formations have differing infrarrot frequencies. Infrared frequencies are also varied. This indicates ZrO_2's optical phononic energy's dependency on crystalline structures [36-38]. ZrO_2 NPs typically rely substantially on crystalline structue [39, 40]. Due to their great strength, durability, enhanced wear resistance, and heat shock resistance, these materials have a wide range of applications [41].
It's also an environmentally friendly, non-toxic, thermally and chemically stable, and cost-effective substance.

MATERIALS AND METHODS

The materials such as Zirconium nitrate, Aloe vera plant extract and DI water were used in the synthesis of

* **R. Gowthami**
✉ rgowthami888@gmail.com

[1-2] Department of Chemistry, Bharath Institute of Higher Education and Research (BIHER), Chennai - 600 073, Tamil Nadu, India

Zirconium oxide (ZrO_2) nanoparticles using green synthesis by microwave irradiation. The precursor materials are of AR and are used directly. Zirconium nitrate was dissolved in 20 ml of DI water and allowed to stir for 10 minutes. Aloe vera plant extract was dissolved in 10 ml of DI water and allow it to stir for 30 minutes. Zirconium nitrate solution is added with *Aloe vera* plant extract and stirred for 35 minutes and then the solution of mixture is irradiated by microwave heating. ZrO_2 nanoparticles powder was obtained and used for further studies.

Characterization techniques

X-ray diffractometer with CuKa radiation (1.5418 Å) (Rigaku, Japan) is used to analyze the structure of the sample. The sample is scanned for a 2θ (20-90o) range with a phase size of 0.02o. For chemical analysis, the FTIR spectrometer, (Spectrum Two FTIR spectrometer) in the 400-4000 cm^{-1} wavenumber range with a resolution of 0.5 cm^{-1}, is used to confirm the chemical bonds in the sample. The sample was absorbed using a double beam spectrophotometer (UV-1800, Shimadzu) with a wavelength range of 200-1000 nm. 1 nm is the resolution. To find the bandgap and defects in the sample, a photoluminescence setup (Model: LS 45 Spectrofluorometer) of 350 nm excitation wavelength and a resolution of 1 nm is used. The sample is non-conducting in the current analysis, which is why a very thin gold layer of around 10 nm is sputter-coated for conduction. Scanning electron microscope (SEM) (Carl Zeiss microscopy ltd, UK & SIGMA) was used to analyse the morphology and composition. Advanced analytical microscopy is provided by Scanning Electron Microscopes (SEM). With its in-lens secondary electron detection, the GEMINI column provides you with unprecedented resolution, contrast and brightness for highly topographical imaging samples. With a high vacuum mode of operation, performing and non-conducting samples are defined as images.

RESULTS AND DISCUSSION

XRD analysis

Powder X-ray diffraction (XRD) studies are distinguished by the structures, crystallinity and crystallite size of the ZrO_2 NPs in the 2θ range of 20-90 ° (Figure 1). The peaks appeared at angles (2 θ) 30.2, 35.1, 50.4, 60.0, 62.9 ° and 74.5 °, due to diffractions of the crystalline planes (101), (110), (200), (211), (202) and (220) of the tetragonal phase ZrO_2 (JCPDS card no. 49-1642). At an annealing temperature of 600°C, the sharp peaks of the XRD pattern suggest the crystallinity of the nanocrystallites. The Scherrer formula was used to measure the crystallite sizes from the (101) peak of the XRD pattern from the FWHM.

$$D = \frac{k\lambda}{\beta \cos\theta}$$

Where D is the crystallite size, λ is the X-ray wavelength (0.15418 nm), β is the angular line width of full width of half-maximum (FWHM) intensity, and θ is Bragg's angle. The crystallite size is found to be 15 nm.

FTIR studies

The transmittance of ZrO_2 nanoparticles in the 500-4000 cm-1 range is shown (Fig.2) by the FTIR spectrum. The 612, 845, 872, 1422, 1620, 2092, 2305, and 2954 cm-1 bands are seen. The absorption band about 2903-1600 cm-1 is O-H bond stretching and bending, meaning water molecule presence. The ~ 1425 cm-1 peak is due to the vibration of C-H bending. The ionic bond peaks of 612 to 872 cm-1 confirm the formation of crystalline ZrO_2 [42].

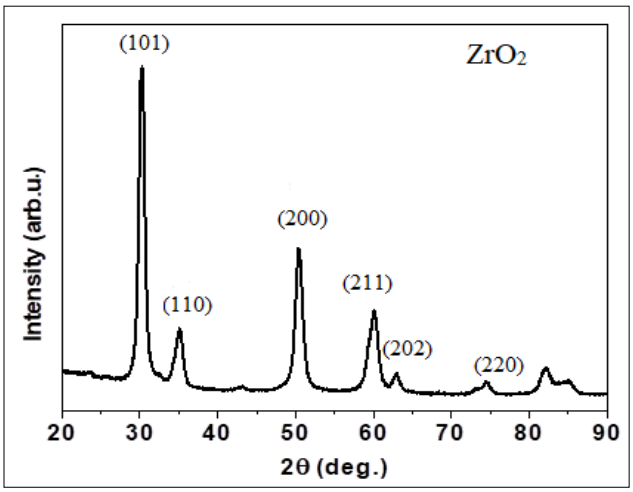

Fig 1 Powder XRD pattern of ZrO_2 NPs

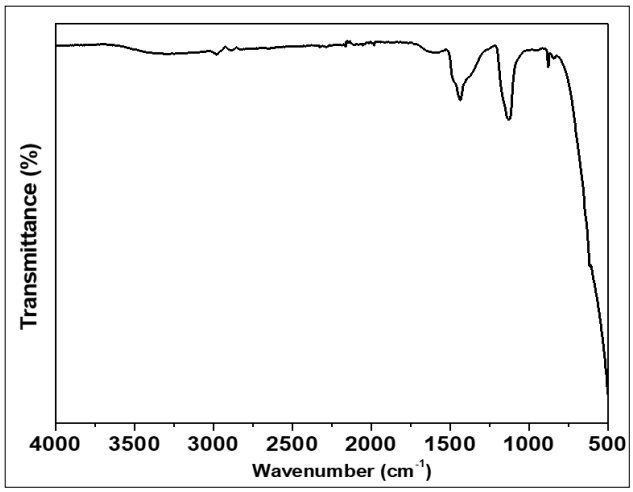

Fig 2 FTIR spectrum of ZrO_2 nanoparticles

SEM analysis

SEM images show the surface morphology of the zirconia nanoparticles (Fig 3). It shows the well-defined formation of the crystallites with different magnifications. The crystallites are agglomerated and formed a cluster. ZrO_2 nanoparticles were aggregated in the form of nano disc/plate shapes.

HR-TEM analysis

Fig. 4 shows the high-resolution transmission electron microscopy (HR-TEM) images of ZrO_2 nanoparticles, which consists of spherical shaped nanoparticles, which are good agreement and evidence of SEM images. Also, the particle sizes of the sample ranging from 12 nm to 15 nm. Average crystallite sizes, obtained from XRD analysis, are consistent with the particle sizes calculated from HR-TEM images.

Optical studies –UV-Visible spectrophotometer

The energy band gap (E_g) of ZrO_2 was obtained from the optical diffuse reflectance spectra (DRS) recorded at room temperature and is shown in Fig. 5. The definition of Kubelka-Munk function is enumerated as follows:

$$\left(F(R)\right) = \alpha = \frac{(1-R)^2}{2R}$$

Where, *F(R)* is Kubelka-Munk function, *α*, the absorbance, *R*, the reflectance. The direct band gap value of the ZrO_2 nanoparticles was observed to be 5.52 eV, which is higher than the reported value of ZrO_2 nanoparticles, i.e., 5.5 eV, suggesting a blue shift, which may be due to the *sp-d* exchange interaction between the localized *d*-electrons of Ni^{2+} ions and band electrons of ZrO_2 nanoparticles [43].

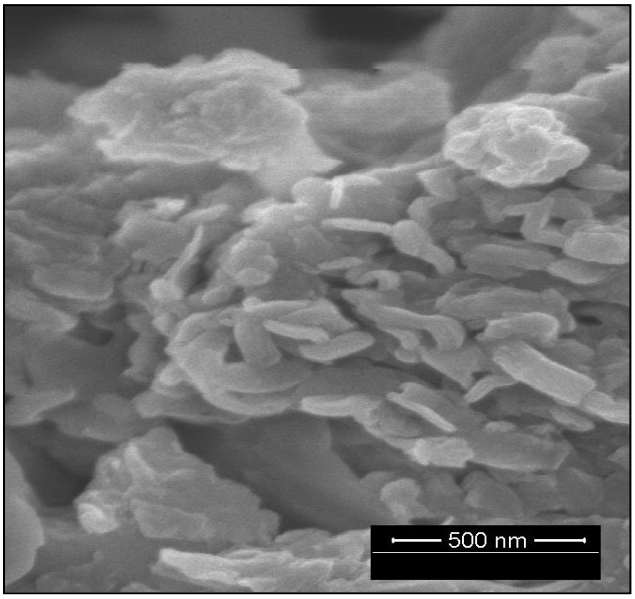

Fig 3 FE-SEM images of ZrO_2 nanoparticles

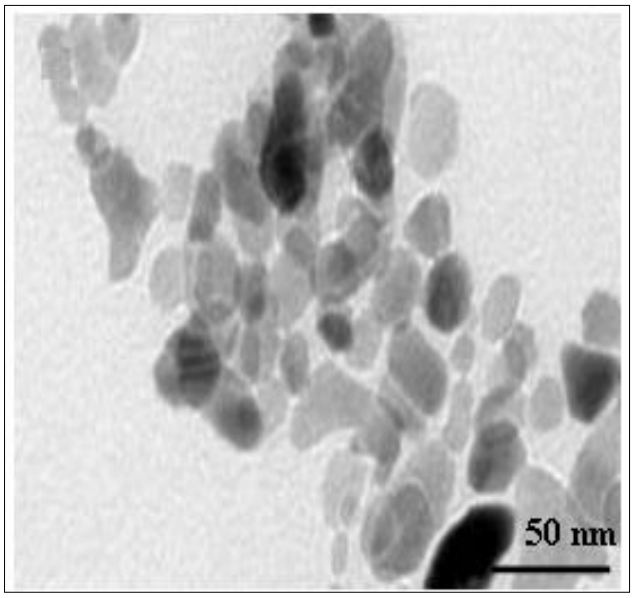

Fig 4 HR-TEM images of ZrO_2 nanoparticles

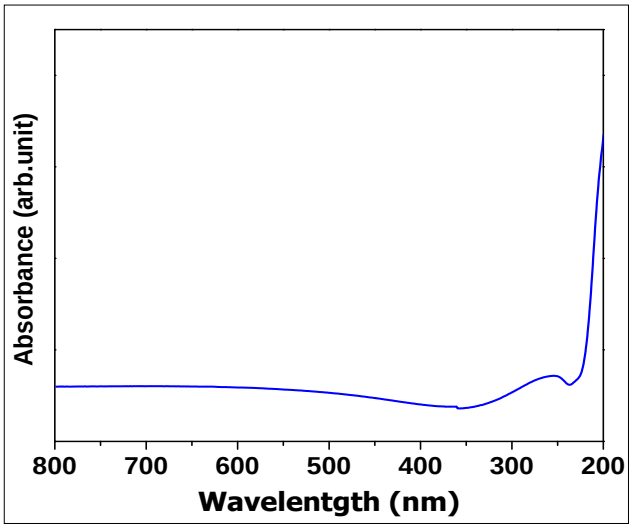

Fig 5 UV-Visible absorbance spectrum of the ZrO_2

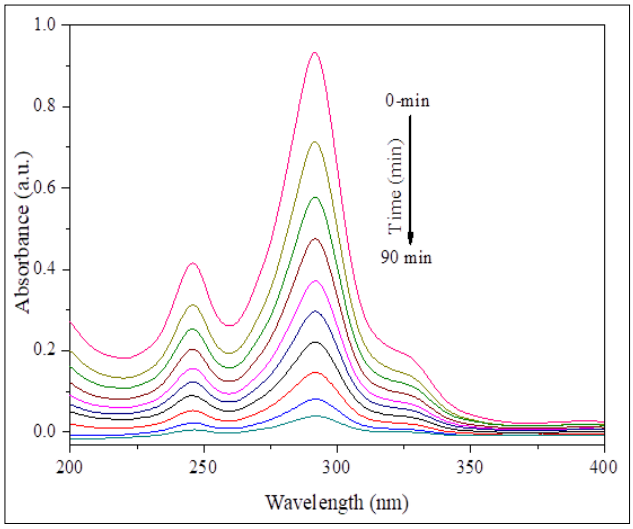

Fig 6 Photocatalytic degradation of MO dye with ZrO_2 catalyst

Photocatalytic studies

Photodegradation of MO as a pollutant is being examined for the efficacy of ZrO_2 NPs 50 mL of MO dye solution (10 mg / L) containing 50 mg of photocatalyst was used for photocatalytic degradation. Suspensions were retained in the dark atmosphere under continuous stirring at RT for 50 minutes prior to detectable irradiation (Fig. 6). During light irradiation, a small amount of the solution is taken at a certain time interval. A UV-Vis spectrophotometer centrifuges each sample and analyses it [44-46]. The separation and transport of charges are significant parameters for efficient photocatalysts. Initially, MO dye adsorption occurs on the photocatalyst surface and then application of visible light to the catalyst adsorbed by the dye leads to the formation of electron-hole pairs. Superoxide anion radicals are created by the interaction of the electron in the conduction band with the adsorbed oxygen molecules over the photocatalyst. Similarly, holes formed in the catalyst VB react with groups of surface hydroxyls. In the final step, in the presence of the photocatalyst, hydroxyl radicals (OH) and superoxide anion radicals (O2 −) react with MO dye, resulting in the degradation of MO dye into smaller degraded products.

CONCLUSION

Plant extract was used to make ZrO_2 nanoparticles in a green. ZrO_2 nanoparticles were made using zirconium, *Aloe vera* plant extract, and DI water. The *Aloe vera* plant extract is applied and agitated in the zirco nium oxynitrate solution, then kept in a microwave oven to pr omote powder formation. Fourier transform infrared (FTIR) spectroscopy, high resolution scanning electron microscopy (HRSEM), UV-Visible spectroscopy and photocatalytic studies were used to study the ZrO_2 nanoparticles. The tetragonal structure of ZrO_2 NPs was indicated in the XRD data. HR-SEM analysis has shown that ZrO_2 nanoparticles are agglomerated with a plate-like structure. UV-Visible absorption tests have shown a 5.51 e. V bandgap for the nanoparticles of ZrO_2. In the MO dye solution, nanoparticles (1g / l) are added and stored in the photoreactor to study the

dye's degradation under visible light. Studies have shown that ZrO_2 nanoparticles effectively degrade the MO dye under visible light irradiation. After 120 min of irradiation, the photocatalytic studies indicated 93.5 % degradation efficiency.

LITERATURE CITED

1. E Murugan, A Siva, Preparation of a novel soluble multi-site phase transfer catalyst and the kinetic study for the C-alkylation of α-pinene. Journal of Molecular Catalysis A: Chemical, 2005, 235 (1-2), 220-229.
2. C. Sambathkumar, R. Ranjithkumar, S. Ezhil Arasi, A. Manikandan, N. Nallamuthu, M. Krishna Kumar, A. Arivarasan, P. Devendran, High-performance nickel sulfide modified electrode material from single source precursor for energy storage application, Journal of Materials Science: Materials in Electronics, 32 (2021) 20058-20070.
3. C. Sambathkumar, V. Manirathinam, A. Manikandan, M. Krishna Kumar, S. Sudhakar, P. Devendran, Solvothermal synthesis of Bi_2S_3 nanoparticles for active photocatalytic and energy storage device applications, Journal of Materials Science: Materials in Electronics, 32 (2021) 20827-20843.
4. V. S. P. Sakthi Sri, A. Manikandan, M. Mathankumar, R. Tamizhselvi, M. George, A. L. Bilgrami, S. A. Al-Zahrani, A. A. P. Khan, Anish Khan, A. M. Asiri, Unveiling the photosensitive, mechanical and magnetic properties of amorphous iron nanoparticles with its application towards decontamination of water and cancer treatment, Journal of Materials Research and Technology, 15 (2021) 99-118.
5. E Murugan, G Vimala, Effective functionalization of multiwalled carbon nanotube with amphiphilic poly(propyleneimine) dendrimer carrying silver nanoparticles for better dispersability and antimicrobial activity, Journal of colloid and interface science, 2011, 357 (2), 354-365.
6. E Murugan, JN Jebaranjitham,Dendrimer grafted core–shell Fe3O4–polymer magnetic nanocomposites stabilized with AuNPs for enhanced catalytic degradation of Rhodamine B–A kinetic study, Chemical Engineering Journal, 2015, 259, 266-276.
7. E Murugan, V Gopi, Amphiphilic multiwalled carbon nanotube polymer hybrid with improved conductivity and dispersibility produced by functionalization with poly (vinylbenzyl) triethylammonium chloride, The Journal of Physical Chemistry C, 2011, 115 (40), 19897-19909.
8. S. Blessi, A. Manikandan, S. Anand, M. M. L. Sonia, V. M. Vinosel, P. Paulraj, Y. Slimani, M.A. Almessiere, M. Iqbal, S. Guner, A. Baykal, Effect of Zinc substitution on the physical and electrochemical properties of mesoporous SnO_2 nanomaterials, Materials Chemistry and Physics, 273 (2021) 125122.
9. A. Alagarsamy, S. Chandrasekaran, A. Manikandan, Green synthesis and characterization studies of biogenic zirconium oxide (ZrO_2) nanoparticles for adsorptive removal of methylene blue dye, Journal of Molecular Structure, 1247 (2022) 131275. Impact Factor: 3.196 (Elsevier)
10. A. Muthukrishnaraj , S. A. Al-Zahrani , A. Al Otaibi , S. S. Kalaivani, A. Manikandan, N. Balasubramanian, A. L. Bilgrami, M. A. R. Ahamed, A. Khan, A. M. Asiri, N. Balasubramanian, Enhanced Photocatalytic Activity of Cu_2O Cabbage/RGO Nanocomposites under Visible Light Irradiation, Polymers, 13 (2021) 1712
11. S. Blessi, A.Manikandan, S.Anand, M. M. L. Sonia, V.M. Vinosel, A. M. Alosaimi, A. Khan, M. A. Hussein, A. M. Asiri, Enhanced electrochemical performance and humidity sensing properties of Al^{3+} substituted mesoporous SnO_2 nanoparticles, Physica E: Low-dimensional Systems and Nanostructures, 133 (2021) 114820.
12. R. Kalidoss, K. Radhakrishnan, A. Manikandan, S.K.Jaganathan, A. Khan, A. M. Asiri, Socio-Economic Demands and Challenges for Non-invasive Disease Diagnosis through Portable Breathalyzer by the Incorporation of 2D Nanosheets and SMO Nanocomposites, RSC Advances, 11 (2021) 21216–21234.
13. K. Geetha, R. Udhayakumar, A. Manikandan, Enhanced magnetic and photocatalytic characteristics of cerium substituted spinel $MgFe_2O_4$ ferrite nanoparticles, Physica B: Physics of Condensed Matter, 615 (2021) 413083.
14. S. S. Al-Jameel, S. Rehman, M. A. Almessiere, F. A. Khan, Y. Slimani, N. S. Al-Saleh, A. Manikandan, E. A. Al-Suhaimi, A. Baykal, Anti-microbial and anti-cancer activities of $MnZnDy_xFe_{2-x}O_4$ ($x \leq 0.1$) nanoparticles, Artificial Cells, Nanomedicine and Biotechnology, 49 (2021) 493-499.
15. P. Annie Vinosha, A. Manikandan, A. Christy Preetha, A. Dinesh, Y. Slimani, M.A. Almessiere, A. Baykal, Belina Xavier, G. Francisco Nirmala, Review on recent advances of synthesis, magnetic properties and water treatment applications of cobalt ferrite nanoparticles and nanocomposites, Journal of Superconductivity and Novel Magnetism, 34 (2021) 995–1018.
16. S. S. Al-Jameel, M. A. Almessiere, F. A. Khan, N. Taskhandi , Y. Slimani, N. S. Al-Saleh, A. Manikandan, E. A. Al-Suhaimi, A. Baykal, Synthesis, Characterization, Anti-Cancer Analysis of $Sr_{0.5}Ba_{0.5}Dy_xSm_xFe_{8-2x}O_{19}$ ($0.00 \leq x \leq 1.0$) Microsphere Nanocomposites, Nanomaterials, 11 (2021) 700.
17. A. P. Subramanian, S. K. Jaganathan, A. Manikandan, K. N. Pandiaraj, N. Gomathi and E. Supriyanto, Recent trends in nano based drug delivery systems for efficient delivery of phytochemicals in chemotherapy, RSC Advances, 6 **(**2016**)** 48294-48314.
18. V. Muthuvignesh, V.J. Reddy, S. Ramakrishna, S. Ray, A. Ismail, M. Mandal, A. Manikandan, S. Seal and S. K. Jaganathan, Electrospinning applications from diagnosis to treatment of diabetes, RSC Advances, 6 (2016) 83638-83655.
19. V. Muthuvignesh, S. K. Jaganathan, A. Manikandan, Nanomaterials as a game changer in the management and treatment of diabetic foot ulcers, RSC Advances, **6** (2016) 114859-114878.
20. M. Vanitha, G. Ramachandran, A. Manikandan, Y. Slimani, M. A. Almessiere, A. Baykal, C. S. Dash, Effect of Sr^{2+} ions substituted nickel ferrite nanoparticles prepared by a simple microwave combustion method, Journal of Superconductivity and Novel Magnetism, 34 (2021) 971-980.
21. SP Ratnayake, M Mantilaka, C Sandaruwan, D Dahanayake, E Murugan, Carbon quantum dots-decorated nano-zirconia: a highly efficient photocatalyst, Applied Catalysis A: General, 2019, 570, 23-30.
22. E Murugan, P Gopinath, V Shanmugayya, N Mathivanan, Antibacterial activity of novel insoluble bead-shaped polymer-supported multiquaternary ammonium salts, Journal of applied polymer science, 2010, 117 (6), 3673-3678
23. E Murugan, I Pakrudheen, Efficient amphiphilic poly (propylene imine) dendrimer encapsulated ruthenium nanoparticles for sensing and catalysis applications, Science of Advanced Materials, 2015, 7 (5), 891-901.

24. E Murugan, JN Jebaranjitham, A Usha Synthesis of polymer-supported dendritic palladium nanoparticle catalysts for Suzuki coupling reaction, Applied Nanoscience, 2012, 2 (3), 211-222
25. E Murugan, JN Jebaranjitham, KJ Raman, A Mandal, D Geethalakshmi, Insoluble dendrimer-grafted poly (vinylimidazole) microbeads stabilized with mono/bimetallic nanoparticle catalysts for effective degradation of malachite green, New Journal of Chemistry, 2017, 41 (19), 10860-10871
26. E Murugan, SS Kumar, KM Reshna, S Govindaraju, Highly sensitive, stable g-CN decorated with AgNPs for SERS sensing of toluidine blue and catalytic reduction of crystal violet, Journal of materials science 2019, 54 (7), 5294-5310
27. E Murugan, M Ariraman, S Rajendran, J Kathirvel, CR Akshata, K Kumar, Core–Shell Nanostructured Fe3O4–Poly(styrene-co-vinylbenzyl chloride) Grafted PPI Dendrimers Stabilized with AuNPs/PdNPs for Efficient Nuclease Activity, ACS omega, 2018, 3 (10), 13685-13693.
28. P Shanmugam, K Rajakumar, R Boddula, RC Ngullie, W Wei, J Xie,Heterogeneous form of poly (4-vinyl pyridine) beads based dendrimer stabilized Ag, Au and PdNPs catalyst for reduction of trypan blue, Materials Science for Energy Technologies, 2019, 2 (3), 532-542.
29. E Murugan, S Santhoshkumar, S Govindaraju, M Palanichamy, Silver nanoparticles decorated g-C3N4: An efficient SERS substrate for monitoring catalytic reduction and selective Hg2+ ions detection, Spectrochimica Acta Part A: Molecular and Biomolecular Spectroscopy, 2021, 246, 119036.
30. S Santhoshkumar, E Murugan, Rationally designed SERS AgNPs/GO/g-CN nanohybrids to detect methylene blue and Hg2+ ions in aqueous solution, Applied Surface Science, 2021, 553, 149544.
31. SP Ratnayake, C Sandaruwan, M Mantilaka, N de Silva, D Dahanayake, U.KWanninayaka, W.R.L.N.Bandara, S.Santhoshkumar, E.Murugan, G.A.J.Amaratunga, K.M. Nalinde Silv, Industrial and environmental significance of photonic zirconia nanoflakes: Influence of boron doping on structure and band states, Journal of Industrial and Engineering Chemistry, 2021, 95, 203-214.
32. I Pakrudheen, AN Banu, E Murugan, Cationic amphiphilic dendrimers with tunable hydrophobicity show in vitro Activity, Environmental Chemistry Letters, 2018, 16 (4), 1513-1519
33. E Murugan, A Rubavathy Jaya Priya, K Janaki Raman, K Kalpana, C R Akshata, S Santhoshkumar, S Govindaraju, Multiwalled carbon nanotubes/gold nanoparticles hybrid electrodes for enzyme-free electrochemical glucose sensor, Journal of nanoscience and nanotechnology, 2019, 19 (12), 7596-7604
34. E Murugan, R Rangasamy, Development of stable pollution free TiO2/Au nanoparticle immobilized green photo catalyst for degradation of methyl orange, Journal of biomedical nanotechnology, 2011, 7 (1), 225-228.
35. E Murugan, G Vimala, Synthesis, characterization, and catalytic activity for hybrids of multi-walled carbon nanotube and amphiphilic poly(propyleneimine) dendrimer immobilized with silver and palladium nanoparticle, Journal of colloid and interface science 2013, 396, 101-111.
36. E Murugan, RL Sherman, HO Spivey, Catalysis by hydrophobically modified poly (propylenimine) dendrimers having quaternary ammonium and tertiary amine functionality, WT Ford, Langmuir, 2004, 20 (19), 8307-8312.
37. S. Blessi, S. Anand, A. Manikandan, M. Maria Lumina Sonia, V. Maria Vinosel, Y. Slimani, M.A. Almessiere, A. Baykal, Influence of Ni substitution on opto-magnetic and electrochemical properties of CTAB capped mesoporous SnO_2 nanoparticles, Journal of Materials Science: Materials in Electronics, Journal of Materials Science: Materials in Electronics, 32 (2021) 7630–7646.
38. T. L. Ajeesha, A. Ashwini, Mary George, A. Manikandan, J. Arul Mary, Y. Slimani, M. A. Almessiere, A. Baykal, Nickel substituted $MgFe_2O_4$ nanoparticles via co-precipitation method for photocatalytic applications, Physica B: Condensed Matter, 606 (2021) 412660.
39. S. Blessi, S. Anand, A. Manikandan, M. M. Lumina Sonia, V. Maria Vinosel, Y. Slimani, M.A. Almessiere, A. Baykal, Structural, optical and electrochemical investigations of Sb substituted mesoporous SnO_2 nanoparticles, Journal of Materials Science: Materials in Electronics, 32 (2021) 4132–4145.
40. R. Kalidoss, K. Radhakrishnan, A. Manikandan, S.K.Jaganathan, A. Khan, A. M. Asiri, Socio-Economic Demands and Challenges for Non-invasive Disease Diagnosis through Portable Breathalyzer by the Incorporation of 2D Nanosheets and SMO Nanocomposites, RSC Advances, 11 (2021) 21216–21234.
41. K. Geetha, R. Udhayakumar, A. Manikandan, Enhanced magnetic and photocatalytic characteristics of cerium substituted spinel $MgFe_2O_4$ ferrite nanoparticles, Physica B: Physics of Condensed Matter, 615 (2021) 413083
42. S. S. Al-Jameel, S. Rehman, M. A. Almessiere, F. A. Khan, Y. Slimani, N. S. Al-Saleh, A. Manikandan, E. A. Al-Suhaimi, A. Baykal, Anti-microbial and anti-cancer activities of $MnZnDy_xFe_{2-x}O_4$ ($x \leq 0.1$) nanoparticles, Artificial Cells, Nanomedicine and Biotechnology, 49 (2021) 493-499.
43. S. Blessi, A.Manikandan, S.Anand, M. M. L. Sonia, V.M. Vinosel, A. M. Alosaimi, A. Khan, M. A. Hussein, A. M. Asiri, Enhanced electrochemical performance and humidity sensing properties of Al^{3+} substituted mesoporous SnO_2 nanoparticles, Physica E: Low-dimensional Systems and Nanostructures, 133 (2021) 114820.
44. A. Muthukrishnaraj , S. A. Al-Zahrani , A. Al Otaibi , S. S. Kalaivani, A. Manikandan, N. Balasubramanian, A. L. Bilgrami, M. A. R. Ahamed, A. Khan, A. M. Asiri, N. Balasubramanian, Enhanced Photocatalytic Activity of Cu_2O Cabbage/RGO Nanocomposites under Visible Light Irradiation, Polymers, 13 (2021) 1712
45. P. A. Vinosha, A. Manikandan, A. S. J. Ceicilia, A. Dinesh, G. F. Nirmala, A. Christy Preetha, Y. Slimani, M.A. Almessiere, A. Baykal, B. Xavier, Review on recent advances of zinc substituted cobalt ferrite nanoparticles: Synthesis characterization and diverse applications, Ceramics International, 47 (2021) 10512-10535.
45. M. George, T.L. Ajeesha, A. Manikandan, Ashwini Anantharaman, R.S. Jansi, E. Ranjith Kumar, Y. Slimani, M.A. Almessiere, A. Baykal, Evaluation of Cu-$MgFe_2O_4$ spinel nanoparticles for photocatalytic and antimicrobial activates, Journal of Physics and Chemistry of Solids, 153 (2021) 110010.